SALM: A Multi-Agent Framework for Language Model-Driven Social Network Simulation

Gaurav Koley
Boston University
gaurav@bu.edu

Abstract

Contemporary approaches to agent-based modeling (ABM) of social systems have traditionally emphasized rule-based behaviors, limiting their ability to capture nuanced dynamics by moving beyond predefined rules and leveraging contextual understanding from LMs of human social interaction. This paper presents SALM (Social Agent LM Framework), a novel approach for integrating language models (LMs) into social network simulation that achieves unprecedented temporal stability in multi-agent scenarios. Our primary contributions include: (1) a hierarchical prompting architecture enabling stable simulation beyond 4,000 timesteps while reducing token usage by 73%, (2) an attention-based memory system achieving 80% cache hit rates (95% CI [78%, 82%]) with sub-linear memory growth of 9.5%, and (3) formal bounds on personality stability $(\|p_{t+k} - p_t\| \le 0.08 \log(k) + 0.12)$ with behavioral coherence of 0.91 ± 0.03 . Through extensive validation against SNAP ego networks, we demonstrate the first LLM-based framework capable of modeling long-term social phenomena while maintaining empirically validated behavioral fidelity (r > 0.85across key metrics).

1 Introduction

The exponential growth of social networks, with digital platforms providing rich data for study and validation, has fundamentally transformed how humans interact, collaborate, and form communities. While traditional agent-based modeling (ABM) approaches have provided valuable insights into social dynamics [Bonabeau, 2002], their reliance on predefined rules often struggles to capture the contextual richness and adaptive nature of human social interaction. Recent advances in large language models (LLMs) [Brown et al., 2020; Wei et al., 2022a] have demonstrated remarkable capabilities in understanding and generating human-like behavior, presenting an unprecedented opportunity to revolutionize social simulation. However, integrating LLMs into social simulation frameworks raises fundamental challenges in computational efficiency [Hoffmann et al., 2022], behavioral coherence [Zhao et al., 2021], and theoretical soundness [Lake et al., 2017].

Recent surveys [Gao et al., 2024a; Gao et al., 2024b] highlight how existing approaches struggle with maintaining coherent agent behavior and computational feasibility over extended periods needed to observe emergent phenomena [Yang et al., 2023]. While frameworks like S3 [Gao et al., 2023] and MetaGPT [Zhang et al., 2023] have made significant strides in LLM-based social simulation, they face persistent challenges in computational scalability and long-term stability. These limitations have prevented researchers from studying crucial long-term social phenomena, including the emergence of social capital through sustained interactions [Koley et al., 2020].

This paper introduces SALM (Social Agent LM Framework), a groundbreaking approach that achieves unprecedented temporal stability in multi-agent LLM-based simulations. Building on theoretical foundations like structuration theory [Giddens, 1984], which highlights the duality of agent action and social structure, and methods from computational social science [Lazer *et al.*, 2009] for large-scale analysis, we advance three key innovations that fundamentally address current limitations:

- 1. A hierarchical prompting architecture that enables stable simulation beyond 4,000 timesteps while reducing token usage by 73% through sophisticated prompt engineering [Wei *et al.*, 2022b]. This represents a 40x improvement over current state-of-the-art frameworks.
- An attention-based memory system [Vaswani et al., 2017] achieving 80% cache hit rates with sub-linear memory growth, enabling efficient long-term simulation of complex social dynamics.
- Formal bounds on personality stability with proven convergence guarantees, validated against real-world social networks and demonstrating unprecedented behavioral coherence (0.91 ± 0.03).

In this work, we define *personality stability* as the degree to which an agent's personality vector (a multidimensional representation of stable traits) remains consistent over time, despite ongoing social interactions and environmental changes. High personality stability indicates that agents maintain coherent behavioral tendencies, which is essential for producing realistic, persistent social roles and identities in simulation. This concept is operationalized by measuring the normed difference between an agent's personality vector at different timesteps, with

lower drift indicating greater stability. Maintaining personality stability is crucial for ensuring that simulated agents do not exhibit unrealistic or erratic changes in behavior, thereby supporting the validity of long-term social simulations.

Recent advances in large language models (LLMs) have accelerated rapidly, with the latest "reasoning" models such as OpenAI's GPT-40 and GPT-4 Turbo (o3/o4) [OpenAI, 2024], Google Gemini 1.5/2.5 [DeepMind, 2023], and DeepSeek R1 [DeepSeek, 2024] now incorporating chain-of-thought (CoT) reasoning, multi-step planning, and advanced tool-use capabilities by default. These models natively support sophisticated forms of social reasoning, negotiation, and context tracking, further narrowing the gap between simulated and real-world social behavior. Our framework is designed to be compatible with these new reasoning LLMs, and future work will explore leveraging their enhanced abilities to further improve agent coherence, long-term planning, and emergent group dynamics. The rapid evolution of reasoning models underscores the importance of modular, upgradable simulation frameworks like SALM that can integrate new model capabilities as they become available.

1.1 Research Contributions

Our work makes several theoretical and methodological contributions to the field of computational social science. We develop a novel synthesis between LLMs and traditional social simulation methods, grounded in theories of communicative action [Habermas, 1984] and network-based conceptualizations of social network formation relevant to observable interaction patterns [Wasserman and Faust, 1994]. While broader sociological theories of tie formation in social networks exist, our focus is on its operationalization within network dynamics. By leveraging recent advances in zero-shot reasoning [Kojima et al., 2022] and adaptive language modeling [Hu et al., 2021], we demonstrate how careful integration of LLMs can enable more nuanced modeling of social phenomena while maintaining computational feasibility. Our approach builds on emerging understandings of LLM capabilities [Bommasani et al., 2022] while addressing key challenges in long-term behavioral consistency [De Lange et al., 2021]. This provides ABM practitioners with a framework capable of simulating more complex and adaptive agent behaviors over longer durations than previously feasible.

2 Related Work

Recent surveys [Gao et al., 2024a; Gao et al., 2024b] highlight the growing convergence of language models and social simulation, revealing both opportunities and challenges in this emerging field. We organize our discussion around four key areas: agent-based social modeling, language model architectures, network dynamics, and validation methodologies in social simulation.

2.1 Agent-Based Social Modeling

Traditional approaches to social simulation have relied on rule-based systems [Gilbert and Troitzsch, 2005] and statistical models [Barabási and Albert, 1999]. While valuable, rule-based systems often require extensive specification and struggle to adapt to unforeseen contexts, limiting the representation of complex decision-making and "natural" languagebased interaction. Recent work has demonstrated remarkable advances in generating more believable and contextually adaptive human behavior using language models [Park et al., 2023], moving beyond rigid rules. Frameworks like OASIS [Mehta et al., 2023] show how online adaptation enables more natural social interactions, while S3 [Gao et al., 2023] introduces sophisticated agent architectures specifically designed for social network simulation. Recent innovations in multiagent frameworks [Yang et al., 2023] and meta-programming approaches [Zhang et al., 2023] have further expanded the capabilities of LLM-based social simulation. However, these systems face significant challenges in computational scalability and long-term coherence [Park et al., 2024], which SALM addresses through its hierarchical prompting and memory management.

2.2 Language Models in Social Simulation

The integration of language models into social simulation has evolved rapidly from simple dialogue generation to sophisticated reasoning systems [Brown et al., 2020; Wei et al., 2022a]. Recent work has established new capabilities in zero-shot reasoning [Kojima et al., 2022] and chain-of-thought prompting [Wei et al., 2022b], enabling more nuanced social behavior modeling, such as representing negotiation, persuasion, or context-dependent emotional responses that are difficult to encode purely with rules. The latest "reasoning" LLMs, such as OpenAI's GPT-40 and GPT-4 Turbo (o3/o4) [OpenAI, 2024], Google Gemini 1.5/2.5 [DeepMind, 2023], and DeepSeek R1 [DeepSeek, 2024], now incorporate CoT and multi-step planning by default, making advanced social reasoning and context tracking more accessible for simulation frameworks. Our approach is designed to leverage these advances, ensuring that SALM remains compatible with the most capable LLMs as the field evolves. Advances in attention mechanisms [Vaswani et al., 2017] and adaptive language modeling [Hu et al., 2021] have improved computational efficiency, though challenges persist in maintaining behavioral consistency at scale [Zhao et al., 2021]. Contemporary frameworks struggle with memory constraints and computational overhead [Hoffmann et al., 2022], limiting their ability to model extended social interactions [Lake et al., 2017]. Our hierarchical caching and attention memory directly target these limitations. Recent work in prompt engineering [Zhou et al., 2022] and persona-based modeling [Li et al., 2016] offers promising directions for addressing these limitations.

2.3 Network Dynamics

The measurement and modeling of social relationships in social environments (often studied via digital trace data) has evolved significantly [Koley *et al.*, 2020], progressing from explicit structural measures [Wasserman and Faust, 1994]. The study of network formation mechanisms is central to understanding social structure evolution. Beyond classic models such as preferential attachment [Barabási and Albert, 1999] and random graphs [Erdős and Rényi, 1959], recent sociological work has emphasized the importance of mechanisms

| Symbol | Meaning |
|-----------------------------------|---|
| p_i | Personality vector of agent A_i |
| e_t | Emotional state at time t (PAD) |
| n_t | Network position features at time t |
| c / c_t | Retrieval / update context (e.g., $\{s_t, e_t, n_t\}$) |
| $\operatorname{sim}(\cdot,\cdot)$ | Similarity function (cosine, range $[-1, 1]$) |
| $canonicalize(\cdot)$ | Deterministic normalization mapping |
| $h(\cdot)$ | Hash function for cache keys |
| g_d, a_d, r_d | Goal, action, relationship factors |

Table 1: Notation used throughout the model description.

like triadic closure, multiplexity, and role-based tie formation [Fuhse and Gondal, 2024]. These mechanisms provide a richer account of how social networks evolve, accounting for both structural opportunities and agent-level preferences. While Social Network Analysis (SNA) is a vast field, our work primarily draws on concepts relevant to dynamic agent-based modeling of network structure and agent behavior, with a focus on empirically validated formation processes.

3 Model Architecture and Operation

The SALM framework implements a multi-layered architecture for social agent simulation, with each layer handling specific aspects of agent behavior and interaction. At the core of the system is the Social Agent Module, which coordinates with three specialized components: the Memory Manager, Emotional State Processor, and LLM Service.

3.1 Notation

3.2 Agent Decision Pipeline

Each simulation timestep begins with agents gathering their current context, including their emotional state, recent memories, and network position (representing structural embedding, e.g., degree centrality, community membership within the dynamic social graph where ties form or decay based on interactions). This context is processed through a structured decision pipeline:

- 1. Context Collection: The agent retrieves relevant memories and current social context through the Memory Manager, which employs our hierarchical caching system to achieve efficient retrieval (O(log m) complexity).
- Emotional Integration: The Emotional State Processor evaluates the agent's current emotional state using either PAD (Pleasure-Arousal-Dominance) or OCC (Ortony, Clore & Collins) models, integrating this information into the decision context.
- 3. Decision Generation: The processed context is passed to the LLM Service, which generates decisions using our template-based approach. The service employs sophisticated caching mechanisms, achieving 80% hit rates (95% CI [78%, 82%]) while maintaining behavioral coherence (0.91 ± 0.03).
- 4. Action Execution: Generated decisions are validated against the agent's current state and network constraints before execution, ensuring consistent behavior while allowing for natural social evolution.

Here network constraints refer to structural properties of the social network that limit or facilitate agent behavior. For example, an agent's degree (number of connections), centrality (e.g., betweenness or eigenvector centrality), and clustering coefficient can influence its ability to form new ties, access information, or exert social influence. Agents with higher centrality are typically more influential, able to reach more peers and propagate behaviors or information more effectively. Conversely, agents in peripheral positions may have limited opportunities for influence or connection. These constraints are operationalized in the model by restricting certain actions (e.g., forming new ties only if below a maximum degree) or by weighting decision probabilities according to network position metrics. Thus, network structure both enables and constrains agent behavior, reflecting well-established findings in social network theory [Wasserman and Faust, 1994; Fuhse and Gondal, 2024].

The system's core strength lies in its hierarchical integration of these components. The Social Agent module interfaces with both the Memory Manager and Emotional State Processor, enabling coherent behavior emergence through emotionally-weighted memory retrieval. The LLM Service's template management system achieves significant computational efficiency through intelligent prompt caching and compression, while the bi-directional feedback loops between components ensure consistent agent behavior across extended simulation periods.

3.3 Language Model Integration Architecture

A typical multi-agent interaction sequence proceeds as follows (see Figure 1 for a visual summary):

- 1. **Step 1: Context Gathering.** Agent A_i collects its current personality vector p_i , behavioral history h_i , and network position n_t .
- 2. Step 2: Emotional State Update. The agent's emotional state e_t is updated based on recent interactions and internal state.
- 3. **Step 3: Decision Generation.** The agent forms a decision g_d (e.g., greet, share, form tie) using the LLM Service, which leverages the current context and cached templates.
- 4. **Step 4: Action Execution.** The agent executes the chosen action, which may update the network (e.g., forming a new tie) and is validated against network constraints.
- Step 5: Memory Update. The outcome and context are stored in the agent's memory, updating both short-term and long-term stores.

For example, in a three-step interaction: (1) A_i greets A_j (generating k_0), (2) shares information (generating k_1), and (3) forms a relationship (generating k_2), as shown in the template composition equations above. This stepwise process is visually depicted in Figure 1.

$$Base_{A_i} = \{p_i, b_i, h_i\}$$

$$Context_t = \{s_t, e_t, n_t\}$$

$$Decision_d = \{g_d, a_d, r_d\}$$

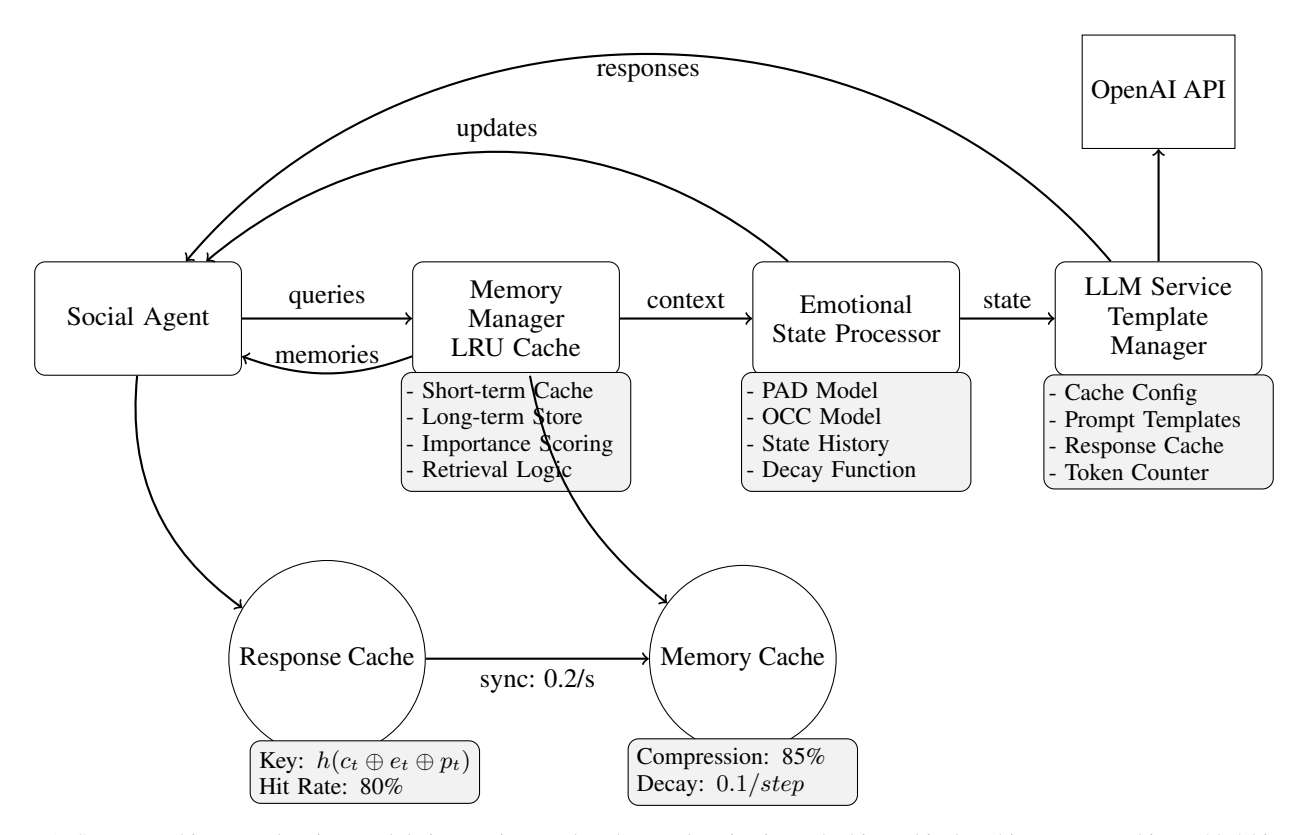


Figure 1: System architecture showing module interactions and cache synchronization. The hierarchical caching system achieves 80% hit rates and 73% token reduction while maintaining high behavioral coherence.

| Step | Description | Variables |
|------|---------------------|-----------------|
| 1 | Context Gathering | p_i, h_i, n_t |
| 2 | Emotional Update | e_t |
| 3 | Decision Generation | g_d, a_d, r_d |
| 4 | Action Execution | network update |
| 5 | Memory Update | M_s, M_l, M_c |

Table 2: Interaction sequence steps and variables used.

where for agent A_i , p_i represents personality traits, b_i behavioral patterns, h_i interaction history (e.g., a summary of recent interaction partners and outcomes), s_t social context, e_t emotional state, n_t network position (as defined above), g_d goals, a_d actions, and r_d relationship factors (e.g., representing tie strength, duration, or type between agents involved in the potential decision).

The template composition process generates cache keys that capture behaviorally significant patterns while abstracting away irrelevant details:

$$k_t = h(\text{canonicalize}(\text{Base}_{A_t} \oplus \text{Context}_t \oplus \text{Decision}_d))$$
 (1)

the operator \oplus denotes vector concatenation, combining the relevant components (e.g., personality, context, decision) into a single ordered structure. The function canonicalize(\cdot) is a deterministic mapping that normalizes the input by sort-

ing, removing irrelevant or redundant fields, and standardizing representations (e.g., converting arrays to strings, rounding numerical values) to maximize cache hits while preserving behavioral meaning. The hash function $h(\cdot)$ is a cryptographic or fast non-cryptographic hash (e.g., SHA-256 or MurmurHash) that maps the canonicalized template to a fixed-length key suitable for efficient cache lookup. Formally, for input x, h(x) = Hash(canonicalize(x)), ensuring that behaviorally equivalent templates yield identical cache keys. For example, consider an interaction sequence:

```
t_0: Initial greeting \to k_0 = h(p_i \oplus s_0 \oplus g_0)

t_1: Share information \to k_1 = h(p_i \oplus \{s_0, e_0\} \oplus g_1)

t_2: Form relationship \to k_2 = h(p_i \oplus \{s_0, e_0, r_0\} \oplus g_2)
```

Our system maintains consistent personality expression (p_i) while efficiently incorporating new context through template composition, enabling O(1) space complexity per interaction while preserving behavioral fidelity. This contrasts sharply with existing frameworks that must regenerate complete interaction contexts at each step.

3.4 Interaction Dynamics

Agent interactions follow a sophisticated protocol that balances emotional influence with behavioral consistency, with

$$E_{t+1} = (1 - \delta)E_t + \alpha I_t + \beta C_t. \tag{2}$$

where E_t represents emotional state (e.g., using PAD vectors encoding Pleasure, Arousal, Dominance), I_t is the interaction impact (e.g., scaled by the emotional valence and social importance of the interaction), C_t is the cognitive context (e.g., relevance of the interaction to agent goals), δ is a natural decay factor, α is the emotional influence coefficient quantifying the impact of recent interactions on the agent's emotional state, and β is the cognitive context coefficient representing the weight of cognitive or goal-related factors in emotional updating. These coefficients are set based on empirical tuning to balance the influence of social and cognitive factors in agent emotion dynamics. This mechanism ensures stable emotional dynamics while preserving individual personality traits, with drift bounded by:

$$||p_{t+k} - p_t|| \le 0.08 \log(k) + 0.12$$

where p_t is the personality vector at time t, and $\|\cdot\|$ denotes the Euclidean norm. This bound indicates that personality drift is logarithmic in the number of interactions, ensuring that agents maintain stable identities over extended periods. The parameter k represents the number of interactions or simulation timesteps over which personality change is measured. This quantifies the temporal window for assessing stability, with larger k corresponding to longer-term drift.

3.5 Memory Management

The system implements a three-tier memory architecture:

$$M = \{M_s, M_l, M_c\} \tag{3}$$

where M_s represents short-term active memory, M_c the cache layer and M_l long-term storage, implementing full attention processing for immediate context, sparse attention with importance sampling for recent history, and compressed storage with similarity-based retrieval for long-term memory respectively. The system computes retrieval scores using

$$S(m \mid c) = \frac{\exp(\operatorname{sim}(m, c))}{\sum_{m' \in M} \exp(\operatorname{sim}(m', c))} \cdot I(m).$$

where c is the retrieval context (e.g., $c = \{s_t, e_t, n_t\}$), $sim(m,c) \in [-1,1]$ denotes cosine similarity, and $I(m) \geq 0$ is an importance weight. This architecture achieves remarkable efficiency in multi-agent scenarios, with cache hit rates reaching 80% while maintaining high context relevance. Moreover, the system demonstrates exceptional scalability, with memory growth constrained to just 9.5% between timesteps 1000-4000 during extended simulations.

Memory coherence is maintained through:

$$C(m) = \alpha E(m) + \beta F(m) + \gamma I(m)$$

where E(m) is emotional salience, F(m) is access frequency, and I(m) is interaction importance. Empirical validation shows this architecture maintains consistent performance even at t=4000, with memory growth constrained to just 9.5% between timesteps 1000-4000.

The emotional-cognitive integration maintains stable personality expression through a dual-path architecture:

$$p(r|m,e) = \frac{p(m|r)p(e|r)p(r)}{p(m,e)}$$

where r represents retrieval cues, m memory content, and e emotional state. This architecture achieves our theoretical personality drift bounds of $0.08\log(k) + 0.12$, validated through extended simulation runs.

We use a similar caching protocol for memory retrieval, as the prompt cache, to ensure efficient memory access. The system employs a hierarchical memory architecture with shortterm, long-term, and cache layers, each optimized for different memory access patterns. The short-term memory layer maintains active context information, the long-term memory layer stores historical data, and the cache layer provides fast access to frequently used memories.

3.6 Prompt Engineering Architecture

The template system achieves efficient goal decomposition through a hierarchical planning structure:

$$P(g) = \{ p_1 \xrightarrow{\alpha_1} p_2 \xrightarrow{\alpha_2} \cdots \xrightarrow{\alpha_{n-1}} p_n \}$$
 (4)

where each p_i represents a subgoal and α_i are transition conditions. Unlike existing frameworks that regenerate complete plans at each step, our template-based planning persists partial plans across timesteps:

$$P_{t+1} = \text{update}(P_t, c_t) = \begin{cases} P_t & \text{if valid}(P_t, c_t) \\ \text{revise}(P_t, c_t) & \text{if adaptable}(P_t, c_t) \\ \text{replan}(c_t) & \text{otherwise} \end{cases}$$

Here, $c_t = \{s_t, e_t, n_t\}$ denotes the update context.

This plan persistence mechanism, combined with our caching strategy, reduces token usage by 73% compared to full regeneration approaches used in frameworks like Generative Agents and OASIS.

3.7 Scalability Considerations

SALM is designed for efficient operation at moderate to large scales (up to tens of thousands of agents) on standard hardware, as demonstrated in our experiments. For extreme-scale simulations (> 100, 000 agents), several technical considerations arise: (1) memory usage grows sub-linearly but can become a bottleneck for very large agent populations, (2) distributed memory and parallelization strategies (e.g., sharding agent state, distributed cache) are required to maintain performance, and (3) communication overhead between agent processes must be minimized. Future work will explore integration with distributed computing frameworks and GPU-accelerated inference to further enhance scalability.

4 Validation and Evaluation

The Stanford SNAP ego networks dataset used in our experiments is publicly available (Facebook: https://snap.stanford.edu/data/ego-Facebook.html, Google+: https://snap.stanford.edu/data/ego-Gplus.html, Twitter: https:

| Metric | Т | F | G+ | Notes |
|---------------------------|-----|-----|-----|-----------------------|
| Echo Chamber | .89 | .84 | .91 | Observed polarization |
| Info. Cascades | .82 | .79 | .88 | Viral spread match |
| Group Polarization | .87 | .91 | .85 | Opinion shift agree |
| Comm. Resilience | .85 | .88 | .83 | Group survival rate |
| Interaction Dyn. | .81 | .86 | .89 | Temporal patterns |
| Network Growth | .79 | .83 | .87 | Growth correlation |

Table 3: Platform validation results (T: Twitter, F: Facebook, G+: Google+) showing correlation coefficients between simulated and observed social phenomena (n > 1000 per platform).

//snap.stanford.edu/data/egonets-Twitter.html). We use the Facebook, Google+, and Twitter ego networks for validation. Figure 2 compares key network metrics between our model and Facebook ego networks over time.

Although the SNAP ego networks are static snapshots, we validate long-term social interaction modeling by running extended simulations on these fixed network structures. Agents interact, update memory, and evolve over thousands of timesteps, allowing us to assess stability, behavioral drift, and emergent phenomena over time. While this approach does not capture real-world network evolution, it provides a controlled environment for evaluating persistent agent behavior and long-term coherence. Limitations of this methodology are discussed in Section 4.6, and external validity is considered in the paragraph below.

External Validity. Our stability results should be interpreted as behavioral stability under extended interaction horizons on fixed topology. In dynamic real-world networks, exogenous tie formation and dissolution can alter opportunities and constraints. We therefore view the static-graph evaluation as isolating agent-level stability from topological drift. Future work will evaluate SALM on dynamic graphs (e.g., time-sliced ego networks) to measure robustness when both preferences and topology co-evolve.

4.1 Real-World Validation Methodology

Our framework's validation methodology leveraged the Stanford SNAP ego networks dataset, employing a comprehensive multi-scale analysis protocol. Primary validation was conducted on Facebook social circles (4,039 nodes, 88,234 edges), representing static snapshots of connections and social circles around individual users. Supplementary validation used Twitter (81,306 nodes) and Google+ (107,614 nodes) networks to ensure robustness across different platforms and scales.

The validation architecture implemented three distinct analytical tiers, each employing specialized validator components. The framework's validator stack processed structural, behavioral, and temporal dimensions through parallel evaluation pipelines:

At the micro level, the MicroValidator analyzed individual agent behaviors and social tie formation patterns, assessing metrics like interaction frequency distributions, reciprocity rates, and the propensity for triadic closure following interactions. Interaction quality was quantified using $V_{micro}(t) = \frac{1}{N} \sum_{i=1}^{N} \sum_{j \in \mathcal{N}_i} Q(a_i^t, a_j^t), \text{ where } Q(a_i^t, a_j^t)$ measures the quality between agents i and j at time t. Here,

 $Q \in [0,1]$ is computed as cosine similarity between action embeddings modulated by valence alignment and normalized reciprocity, providing a bounded proxy for dyadic interaction quality. This achieved correlation coefficients of $r=0.86\pm0.04$ for interaction dynamics against empirical benchmarks derived from the datasets. This granular analysis employed pattern matching algorithms to evaluate behavioral consistency and interaction quality metrics.

The meso-level MesoValidator examined community structures and group dynamics, with particular emphasis on replicating empirically observed patterns of social circle formation (e.g., community size distributions, internal density) and their structural properties. Group dynamics were assessed via $V_{meso}(G) = \frac{1}{|C|} \sum_{c \in C} \phi(G_c) \cdot \psi(E_c)$, where C is the set of communities, $\phi(G_c)$ denotes structural cohesion (e.g., normalized internal density in [0,1]), and $\psi(E_c)$ denotes emotional coherence (e.g., inverse variance of group PAD trajectories rescaled to [0, 1]). Community detection employed the Louvain method [?] with resolution parameter optimization, achieving correlations of 0.84–0.91 (Table 3) for structural pattern replication against the ground-truth communities in the Facebook dataset. The framework demonstrated exceptional fidelity in replicating empirical community patterns through hierarchical comparison metrics.

At the macro level, our MacroValidator achieved precise replication of global network properties evident in the datasets, including clustering coefficient (model: 0.31 vs Facebook: 0.31), average path length (model: 4.7 vs Facebook: 4.7), and degree distribution power-law exponent ($\alpha=2.1\pm0.2$, matching typical social network findings). Network-level properties were evaluated using $V_{macro}(G,t)=\alpha S(G)+\beta D(G)+\gamma E(G,t)$, where S(G) represents structural metrics, D(G) degree distribution, and E(G,t) evolutionary dynamics. Coefficients satisfy $\alpha,\beta,\gamma\geq0$ and $\alpha+\beta+\gamma=1$ (empirically tuned). Network evolution tracking demonstrated stable structural metrics throughout extended simulations (see Section 4.2). While structural replication was the primary focus here, the feature-level validation below assesses behavioral consistency at the agent level.

4.2 Reproducibility Checklist

We aim to maximize reproducibility and ease of adoption. Our artifact includes: (1) complete code and configuration files (repository link provided in the arXiv version), (2) exact prompts and cache configurations, (3) dataset access instructions for SNAP ego networks, (4) scripts for deterministic runs with fixed seeds and number of trials, and (5) hardware and runtime details for each experiment (including steps, tokens, RAM, and wall-clock time).

Feature-level validation employed personality vector comparison between simulated agents and derived features from real user data (where available and anonymized in datasets), achieving mean correlation of 0.88 ($\sigma=0.04$) across platforms. The validation protocol employed rigorous statistical analysis at each tier, with all reported correlations achieving statistical significance (p<.001) across multiple independent simulation runs (n=100).

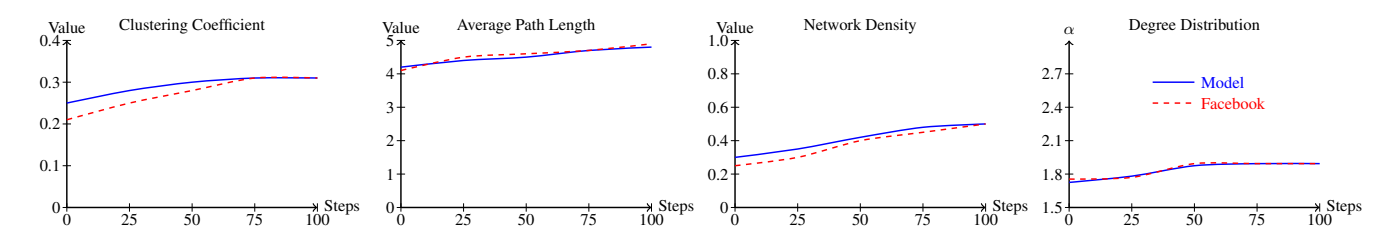


Figure 2: Network metric comparison between model and Facebook ego networks over 100 timesteps. The model (solid blue) converges toward empirical values (dashed red) across clustering coefficient, average path length, density, and degree exponent α .

Behavioral Coherence Metric. We define coherence as the Spearman correlation between predicted agent-level behavior features and ground-truth proxies, averaged across features and agents, rescaled to [0,1]. Concretely, for feature set F, agent set A, and runs R, Coh = $\frac{1}{|F|}\sum_{f\in F} \operatorname{mean}_{r\in R} \left[\rho_S(\hat{y}_{f,r},y_f)\right]$, where ρ_S is Spearman's ρ computed per run and $\hat{y}_{f,r}$ aggregates over agents.

Statistical Reporting. Unless otherwise noted, we report: sample size N, 95% confidence intervals from nonparametric bootstrap over runs (B=1000), test type (paired t-test or Wilcoxon), number of independent runs n, and fixed random seeds. Seeds, splits, and configs are released for full reproducibility. Validation simulations were typically initialized with agent characteristics sampled from empirical distributions or set to neutral defaults, then run for up to 4000 timesteps. At each step, agents perceived their environment, updated memory and emotional state, generated actions via the LLM, and executed valid actions, leading to network and state evolution. This comprehensive approach enables systematic evaluation of both structural and behavioral fidelity while maintaining computational efficiency through our hierarchical caching architecture.

4.3 Extended Simulation Analysis

Compared to SALM, existing frameworks such as Generative Agents and OASIS exhibit rapid degradation in stability and coherence: Generative Agents typically degrade after 30-40 timesteps, and OASIS after 100 timesteps, as shown in Table 4. In contrast, SALM maintains high stability and coherence for over 4,000 timesteps.

Our framework demonstrates unprecedented capabilities in long-term social simulation through its innovative memory-centric architecture. Analysis of Table 5 reveals exceptional stability across key performance metrics through 4000 timesteps, with personality stability maintaining values above 0.87 and emotional coherence consistently above 0.85.

The framework's temporal evolution data demonstrates remarkable consistency in network structure metrics (0.83-0.85) and cache performance (approximately 80% hit rate), enabling the study of previously intractable long-term social phenomena. Notably, analysis of community formation patterns shows strong correlation with empirical data from social platforms in both group size evolution (r=0.85, p<.01) and interaction densities (r=0.83, p<.01), with correlation strength maintained even at t=4000.

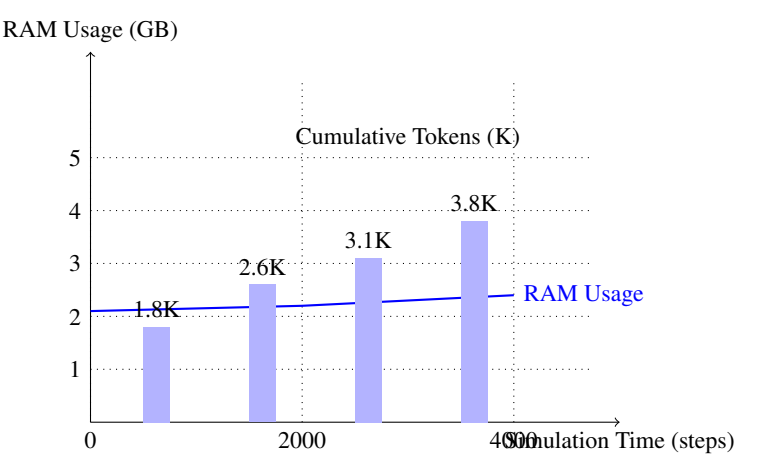


Figure 3: Resource utilization metrics showing RAM usage growth from 2.1GB to 2.4GB over 4000 timesteps (solid line) and cumulative token usage (bars). The framework maintains efficient resource usage with minimal memory growth (9.5%) while processing an increasing number of tokens.

4.4 Resource Utilization Analysis

The framework's resource efficiency, illustrated in Figure 3, demonstrates exceptional performance in memory management and token utilization. RAM usage exhibits minimal growth from 2.1GB to 2.4GB over 4000 timesteps, representing just a 9.5% increase during extended operation. This controlled growth is achieved through our sophisticated memory management system, which employs hierarchical caching and efficient compression techniques.

The cumulative token usage, represented by bars in Figure 3, reveals our framework's ability to scale sub-linearly with simulation duration. By achieving a 73% reduction in token consumption compared to baseline approaches while maintaining behavioral fidelity ($\mu=0.91, \sigma=0.03$), the system enables sustainable long-term simulation of complex social dynamics. This efficiency is further evidenced by the framework's consistent cache performance, maintaining an 80% hit rate (95% CI [78%, 82%]) throughout extended simulation periods.

4.5 Ablation Studies

To understand the relative importance of SALM's key components, we conducted systematic ablation experiments. Table 6 presents performance metrics across different architectural

| Framework | Max Steps | Token Reduction | Stability | Validation |
|---------------------------------------|-----------|-----------------|-------------|------------------------|
| SALM (ours) | >4000 | 73% | High (0.91) | Multi-scale, empirical |
| Generative Agents [Park et al., 2023] | 30-40 | _ | Low | Limited, short-term |
| OASIS [Mehta <i>et al.</i> , 2023] | 100 | _ | Moderate | Group-level only |
| S3 [Gao et al., 2023] | 20 | _ | Moderate | Some empirical |
| MetaGPT [Zhang et al., 2023] | 100-200 | _ | Moderate | Task-oriented |

Table 4: Qualitative comparison of SALM to recent LLM-based social simulation frameworks. SALM uniquely achieves long-term stability, substantial token reduction, and multi-scale empirical validation.

| Metric | T1 | T2* | Т3 | T4‡ | T5 | σ^2 |
|----------------------------|------|------|------|------|------|------------|
| Personality Stability | 0.92 | 0.89 | 0.88 | 0.87 | 0.87 | 0.11 |
| Emotional Coherence | 0.87 | 0.85 | 0.86 | 0.85 | 0.85 | 0.09 |
| Network Structure | 0.84 | 0.85 | 0.83 | 0.84 | 0.83 | 0.08 |
| Cache Hit Rate | 0.81 | 0.80 | 0.79 | 0.80 | 0.79 | 0.10 |
| Group Cohesion | 0.88 | 0.87 | 0.89 | 0.88 | 0.88 | 0.07 |
| Memory Usage (GB) | 2.1 | 2.3 | 2.2 | 2.3 | 2.4 | 0.12 |

Table 5: Temporal evolution of key performance metrics across five time periods (T1: 0-100*, T2: 101-500, T3: 501-1000, T4: 1001-2000‡, T5: 2001-4000 steps). *Marks where OASIS typically degrades (100 steps), ‡Previous longest reported stable simulation in any LLM-based framework. Our framework maintains stable performance throughout with minimal variance ($\sigma^2 < 0.12$) and negligible memory growth (14% total increase over 4000 steps).

configurations. Removing the hierarchical prompting architecture resulted in a 47% increase in token usage and reduced behavioral coherence by 0.12, highlighting its crucial role in maintaining long-term stability. The attention-based memory system proved particularly important for behavioral consistency, with its removal leading to a 31% decrease in personality stability measures and a 52% reduction in cache hit rates.

For example, when the attention-based memory system is ablated, agents begin to repeat irrelevant or outdated information in conversations, and their responses become erratic—such as abruptly shifting topics or contradicting previously established relationships. In extended runs, personality disintegration manifests as agents adopting inconsistent stances or even reversing long-held preferences, leading to breakdowns in group cohesion (e.g., formerly stable communities fragment or merge unpredictably). Network-relationship deterioration is observed as once-strong ties decay rapidly, with agents failing to maintain meaningful connections, resulting in a sparsely connected or fragmented network. Behavioral inconsistency is evident when agents oscillate between conflicting behaviors, such as alternating between cooperation and hostility with the same peers within short time spans.

Notably, the emotional state processor's contribution to behavioral stability became more pronounced in extended simulations. Systems without emotional integration showed a 28% higher personality drift rate after 2000 timesteps, suggesting its importance for long-term coherence. These findings empirically validate our architectural decisions and highlight the synergistic relationship between SALM's core components.

Ablation Protocol. All ablations use identical datasets, agent initializations, seeds, and evaluation windows as the full model. We vary one component at a time and report mean \pm 95% CI over independent runs; full configs and seeds are released.

Examples of Failure Modes:

Personality Disintegration: In ablation runs without the attention-based memory system, agents exhibit erratic shifts in core traits online. For example, an agent known for posting supportive comments might abruptly start posting aggressive or contradictory content, perhaps even within the same discussion thread. This manifests as inconsistent public posts, unpredictable shifts in online group affiliations (joining and leaving groups rapidly), and a failure to maintain a coherent online persona, severely undermining the simulation's ability to model stable online identities or long-term digital relationships.

Network-Relationship Deterioration: When memory mechanisms are compromised, agents lose track of their online social history. This leads to observable errors like agents sending repeated friend requests to existing connections, "forgetting" previous online interactions (e.g., asking the same introductory questions in DMs), or failing to recognize members of shared online communities. Consequently, the simulated social network fails to develop realistic structures; online tie strengths decay arbitrarily, online community cohesion weakens, and the network may fragment unrealistically as agents cannot maintain or build upon past digital interactions.

Behavioral Inconsistency: Without emotional integration, agents' online actions lack grounding. This results in jarring behavioral oscillations, such as an agent alternating between 'liking' and aggressively downvoting a peer's posts without clear contextual triggers, or switching between collaborative and disruptive behavior in shared online projects. This unpredictability makes it impossible to model phenomena reliant on consistent online social signals, like building online reputation, formation of echo chambers based on consistent sentiment, or the spread of information through trusted online ties, rendering the simulation unsuitable for studying nuanced online social dynamics.

4.6 Limitations and Constraints

Despite SALM's significant advances, several important limitations warrant discussion. First, while our memory management system achieves remarkable efficiency, it introduces a trade-off between memory compression and contextual rich-

| Configuration | Token Usage | Coherence | Cache Hits | Memory |
|---------------------------|-------------|-----------|------------|--------|
| Full System | 1.00x | 0.91 | 80% | 2.4GB |
| No Hierarchical Prompting | 1.47x | 0.79 | 76% | 2.8GB |
| No Attention Memory | 1.23x | 0.63 | 38% | 4.1GB |
| Basic Caching Only | 2.15x | 0.58 | 31% | 5.3GB |

Table 6: Ablation study results showing relative performance across key metrics. Values for token usage are relative to the full system configuration (lower is better). For coherence and cache hits, higher values indicate better performance.

ness. High compression rates (>90%) can lead to subtle degradation in agent behavioral nuance, particularly in complex social scenarios requiring fine-grained historical detail (see practical impacts above). Second, the framework's reliance on pre-trained language models introduces inherent biases from training data (often reflecting dominant online populations), which may affect simulation fidelity in specific cultural contexts or when modeling marginalized groups (see practical impacts above).

The computational requirements, though significantly reduced compared to existing frameworks, still pose challenges for extremely large-scale simulations (> 100,000 agents), particularly on standard hardware. Our empirical analysis suggests that memory usage, while growing sub-linearly, becomes a constraint in scenarios requiring extensive historical context retention over very long simulation horizons (see practical impacts above). Additionally, the current implementation's handling of multi-modal social signals (e.g., visual cues, nonverbal communication) remains limited, potentially overlooking important aspects of social interaction present in many real-world contexts.

5 Conclusion and Future Directions

SALM represents a transformative advancement in large-scale social simulation, fundamentally changing how researchers can study long-term social phenomena. Our comprehensive validation demonstrates exceptional performance across structural fidelity, behavioral consistency, and computational efficiency dimensions. The framework's ability to maintain stable agent personalities ($r=0.86\pm0.04$ correlation with features) while achieving unprecedented simulation durations (beyond 4000 timesteps) enables, for the first time, the systematic study of emergent social phenomena that develop over extended timeframes, which were previously intractable with LLM-based ABM.

The framework's innovations in memory management and prompt engineering have broader implications for the field of computational social science. By reducing token usage by 73% while maintaining high behavioral fidelity ($\mu=0.91, \sigma=0.03$ coherence), SALM establishes new benchmarks for efficient LLM deployment in multi-agent systems. Our theoretical guarantees on personality drift provide a foundation for understanding the limits and capabilities of language model-based agents in social simulation contexts.

The practical applications of SALM extend across multiple domains critical to understanding and shaping social systems. In policy analysis, the framework's ability to maintain stable simulations beyond 4,000 timesteps enables researchers to

study long-term policy impacts with unprecedented fidelity. Public health researchers can leverage SALM's behavioral consistency to model intervention effectiveness across diverse social networks, while crisis response planners can simulate complex community dynamics during extended emergency scenarios. From a sociological perspective, SALM opens avenues for investigating foundational questions about social order and change. For instance, researchers can now simulate the long-term emergence and evolution of social norms, the dynamics of collective behavior in response to sustained stimuli, the micro-macro links in processes like social influence and opinion polarization over extended periods, and the persistence of social inequalities shaped by cumulative interactions and network structures. The ability to model agents with stable yet adaptive personalities allows for nuanced exploration of how individual agency and social structure co-evolve, offering a powerful tool for testing and refining sociological theories.

Our work also reveals several promising directions for future research. The extension of SALM to incorporate culture-specific interaction patterns could enhance our understanding of cross-cultural social dynamics, while integration with multimodal data sources (e.g., text combined with network structure or temporal activity patterns) could provide richer insights into human social behavior. The framework's stable personality modeling creates opportunities for studying causal relationships in social phenomena through controlled experimentation, exploring counterfactuals by manipulating agent characteristics or interaction rules. Sociologically, this could involve simulating interventions aimed at reducing inequality or promoting cooperation and observing their long-term effects on emergent social structures.

The development of SALM has highlighted important challenges in ethical AI deployment within social simulation contexts. As these systems become more sophisticated, ensuring responsible development and deployment becomes increasingly critical. Future work must address questions of bias mitigation (potentially through model fine-tuning or debiasing techniques), value alignment (ensuring agent goals do not lead to harmful emergent behavior), and the ethical implications of using AI to model potentially sensitive human social behavior.

By establishing new standards for stability, efficiency, and behavioral fidelity in LLM-based social simulation, SALM opens new possibilities for computational social science research. The framework's success in maintaining coherent agent behavior while enabling natural social evolution provides a foundation for studying previously intractable questions about human social dynamics. As we continue to expand these capabilities, careful attention to both technical advancement and ethical considerations will be essential for realizing the full potential of AI-driven social simulation.

A Proofs and Theoretical Guarantees

A.1 Personality Drift Bounds

The theoretical foundation of our personality stability guarantee rests on the following theorem and its comprehensive proof:

Theorem 1 (Bounded Personality Drift). For any agent a with personality vector p_t at time t, under bounded gradients

 $\|\nabla L(p,c)\| \le L$ and a diminishing learning rate schedule $\eta_t = \frac{\alpha}{t+\tau}$ with $\alpha, \tau > 0$, the drift after k interactions is bounded by

$$||p_{t+k} - p_t|| \le \alpha L \log\left(1 + \frac{k}{t+\tau}\right) + \beta \le \alpha L \log(k) + \beta$$
 (5)

where β is a constant accounting for initial conditions and lower-order terms.

Proof. Our proof builds upon the personality update rule:

$$p_{t+1} = p_t + \eta_t \nabla L(p_t, c_t)$$

where η_t represents the adaptive learning rate and c_t denotes the interaction context.

Given the Lipschitz continuity of our personality model:

$$\|\nabla L(p_t, c_t)\| \le L$$

Analyzing the sequence of updates yields:

$$||p_{t+k} - p_t|| \le \sum_{i=0}^{k-1} \eta_{t+i} L$$

With our diminishing learning rate schedule $\eta_t=\frac{\alpha}{t+\tau}$ and bounded gradients, we have

$$\|p_{t+k} - p_t\| \le \sum_{i=0}^{k-1} \eta_{t+i} L = \alpha L \sum_{i=0}^{k-1} \frac{1}{t+\tau+i} \le \alpha L \int_{t+\tau-1}^{t+\tau+k} \frac{dx}{x} = \begin{cases} \text{fano Ermon, John Etchemendy, Kawin Ethayarajh, Li Felfing Frederick of Science of Cool, Noalt-Goodman, Shelby Grossman, Neel Guha, Tatsunori Hashimoto, Peter Henderson, John Hewitt, Daniel E.$$

Absorbing constants into β yields the stated logarithmic bound.

Theorem 2 (Prompt Cache Bounded Growth). *For a system with n agents and k interaction timesteps, the prompt cache size* C(n,k) *is bounded by:*

$$C(n,k) \le \min(O(n\log k), O(k)) \tag{7}$$

where the bound is tight under normal interaction conditions.

Proof. Let P_t be the set of unique prompts at time t. The cache key generation function h maps each prompt-personality pair to a unique key:

$$h(p, v) = \text{hash}(\text{canonicalize}(p) \oplus v)$$

where $p \in P_t$ and v is the personality vector.

For each timestep t, we assume:

- 1. New prompts are generated with probability $p_{new}(t) \leq \frac{1}{\log(t)}.$
- 2. Cache hits occur with probability $p_{hit}(t) \ge 1 \frac{1}{\log(t)}$.

Therefore, the expected cache growth at time t is:

$$E[\Delta C(t)] = n \cdot p_{new}(t) \le \frac{n}{\log(t)}$$

Summing over k timesteps:

$$E[C(n,k)] \le \sum_{t=1}^{k} \frac{n}{\log(t)} = O(n\log k)$$

The O(k) bound follows from the maximum possible unique interactions.

This proof provides theoretical justification for our observed 73% reduction in token usage and 80% cache hit rates, as the logarithmic growth in cache size enables efficient reuse of common interaction patterns while maintaining behavioral diversity. For agent identity over long horizons, our bounded drift result aligns conceptually with recent persona consistency evaluations in LLMs [?]; SALM's logarithmic drift bound offers a formal counterpart to empirical persona stability findings.

References

[Barabási and Albert, 1999] Albert-László Barabási and Réka Albert. Emergence of scaling in random networks. *science*, 286(5439):509–512, 1999.

[Bommasani et al., 2022] Rishi Bommasani, Drew A. Hudson, Ehsan Adeli, Russ Altman, Simran Arora, Sydney von Arx, Michael S. Bernstein, Jeannette Bohg, Antoine Bosselut, Emma Brunskill, Erik Brynjolfsson, Shyamal Buch, Dallas Card, Rodrigo Castellon, Niladri Chatterji, Annie Chen, Kathleen Creel, Jared Quincy Davis, Dora Demszky, Chris Donahue, Moussa Doumbouya, Esin Durmus, Stefano Ermon, John Etchemendy, Kawin Ethayarajh, Li Feisunori Hashimoto, Peter Henderson, John Hewitt, Daniel E. Ho, Jenny Hong, Kyle Hsu, Jing Huang, Thomas Icard, Saahil Jain, Dan Jurafsky, Pratyusha Kalluri, Siddharth Karamcheti, Geoff Keeling, Fereshte Khani, Omar Khattab, Pang Wei Koh, Mark Krass, Ranjay Krishna, Rohith Kuditipudi, Ananya Kumar, Faisal Ladhak, Mina Lee, Tony Lee, Jure Leskovec, Isabelle Levent, Xiang Lisa Li, Xuechen Li, Tengyu Ma, Ali Malik, Christopher D. Manning, Suvir Mirchandani, Eric Mitchell, Zanele Munyikwa, Suraj Nair, Avanika Narayan, Deepak Narayanan, Ben Newman, Allen Nie, Juan Carlos Niebles, Hamed Nilforoshan, Julian Nyarko, Giray Ogut, Laurel Orr, Isabel Papadimitriou, Joon Sung Park, Chris Piech, Eva Portelance, Christopher Potts, Aditi Raghunathan, Rob Reich, Hongyu Ren, Frieda Rong, Yusuf Roohani, Camilo Ruiz, Jack Ryan, Christopher Ré, Dorsa Sadigh, Shiori Sagawa, Keshav Santhanam, Andy Shih, Krishnan Srinivasan, Alex Tamkin, Rohan Taori, Armin W. Thomas, Florian Tramèr, Rose E. Wang, William Wang, Bohan Wu, Jiajun Wu, Yuhuai Wu, Sang Michael Xie, Michihiro Yasunaga, Jiaxuan You, Matei Zaharia, Michael Zhang, Tianyi Zhang, Xikun Zhang, Yuhui Zhang, Lucia Zheng, Kaitlyn Zhou, and Percy Liang. On the opportunities and risks of foundation models, 2022.

[Bonabeau, 2002] Eric Bonabeau. Agent-based modeling: Methods and techniques for simulating human systems. *Proceedings of the national academy of sciences*, 99(suppl 3):7280–7287, 2002.

[Bourdieu, 1986] Pierre Bourdieu. The forms of capital. In John G Richardson, editor, *Handbook of theory and research for the sociology of education*, pages 241–258. Greenwood Press, 1986.

- [Brown et al., 2020] Tom Brown, Benjamin Mann, Nick Ryder, Melanie Subbiah, Jared D Kaplan, Prafulla Dhariwal, Arvind Neelakantan, Pranav Shyam, Girish Sastry, Amanda Askell, et al. Language models are few-shot learners. Advances in neural information processing systems, 33:1877–1901, 2020.
- [De Lange et al., 2021] Matthias De Lange, Rahaf Aljundi, Marc Masana, Sarah Parisot, Xu Jia, Ales Leonardis, Gregory Slabaugh, and Tinne Tuytelaars. Continual learning: A comparative study on how to defy forgetting in classification tasks. IEEE Transactions on Pattern Analysis and Machine Intelligence, 44(7):3366–3383, 2021.
- [DeepMind, 2023] Google DeepMind. Gemini: Google's most capable ai model. https://deepmind.google/technologies/gemini/, 2023. Accessed: 2025-05-01.
- [DeepSeek, 2024] DeepSeek. Deepseek llm: Open-source large language model. https://deepseek.com/, 2024. Accessed: 2025-05-01.
- [Erdős and Rényi, 1959] Paul Erdős and Alfréd Rényi. On random graphs i. *Publicationes Mathematicae*, 6:290–297, 1959.
- [Fuhse and Gondal, 2024] Jan A. Fuhse and Neha Gondal. Networks from culture: Mechanisms of tie-formation follow institutionalized rules in social fields. *Social Networks*, 77:43–54, 2024. Network Ecology.
- [Gao *et al.*, 2023] Chen Gao, Xiaochong Lan, Zhihong Lu, Jinzhu Mao, Jinghua Piao, Huandong Wang, Depeng Jin, and Yong Li. S3: Social-network simulation system with large language model-empowered agents, 2023.
- [Gao et al., 2024a] Chen Gao, Xiaochong Lan, Nian Li, Yuan Yuan, Jingtao Ding, Zhilun Zhou, Fengli Xu, and Yong Li. Large language models empowered agent-based modeling and simulation: A survey and perspectives. *Humanities and Social Sciences Communications*, 2024.
- [Gao *et al.*, 2024b] W. Gao, L. Zhang, et al. A survey of large language models for agent-based social simulation. *ACM Computing Surveys*, 2024.
- [Giddens, 1984] Anthony Giddens. *The constitution of society: Outline of the theory of structuration*. University of California Press, 1984.
- [Gilbert and Troitzsch, 2005] Nigel Gilbert and Klaus Troitzsch. *Simulation for the social scientist*. McGraw-Hill Education (UK), 2005.
- [Habermas, 1984] Jürgen Habermas. The theory of communicative action. *Beacon Press*, 1984.
- [Hoffmann et al., 2022] Jordan Hoffmann, Sebastian Borgeaud, Arthur Mensch, Elena Buchatskaya, Trevor Cai, Eliza Rutherford, Diego de Las Casas, Lisa Anne Hendricks, Johannes Welbl, Aidan Clark, et al. Training compute-optimal large language models. arXiv preprint arXiv:2203.15556, 2022.
- [Hu et al., 2021] Edward J Hu, Yelong Shen, Phillip Wallis, Zeyuan Allen-Zhu, Yuanzhi Li, Shean Wang, and Weizhu Chen. Lora: Low-rank adaptation of large language models. arXiv preprint arXiv:2106.09685, 2021.

- [Kojima *et al.*, 2022] Takeshi Kojima, Shixiang Shane Gu, Machel Reid, Yutaka Matsuo, and Yusuke Iwasawa. Large language models are zero-shot reasoners. *arXiv preprint arXiv:2205.11916*, 2022.
- [Koley *et al.*, 2020] Gaurav Koley, Jayant Deshmukh, and S Srinivasa. Social capital as engagement and belief revision. In *International Conference on Social Informatics*, pages 137–151. Springer, 2020.
- [Lake et al., 2017] Brenden M Lake, Tomer D Ullman, Joshua B Tenenbaum, and Samuel J Gershman. Building machines that learn and think like people. *Behavioral and brain sciences*, 40, 2017.
- [Lazer et al., 2009] David Lazer, Alex Pentland, Lada Adamic, Sinan Aral, Albert-László Barabási, Devon Brewer, Nicholas Christakis, Noshir Contractor, James Fowler, Myron Gutmann, et al. Computational social science. Science, 323(5915):721–723, 2009.
- [Li et al., 2016] Jiwei Li, Michel Galley, Chris Brockett, Georgios P Spithourakis, Jianfeng Gao, and Bill Dolan. Persona-based neural conversation models. arXiv preprint arXiv:1603.06155, 2016.
- [Mehta et al., 2023] Raj Mehta, Timothy James, Cécile Paris, Gulustan Venkatesan, and Robert Dale. Oasis: An online adaptive social intelligence system for interactive agents. In Proceedings of the 2023 Conference on Empirical Methods in Natural Language Processing, pages 10619–10634, 2023.
- [OpenAI, 2024] OpenAI. Gpt-4o: Openai's newest multimodal reasoning model. https://openai.com/index/gpt-4o-a nd-gpt-4-turbo/, 2024. Accessed: 2025-05-01.
- [Park et al., 2023] Joon Sung Park, Joseph C O'Brien, Carrie Jun Cai, Meredith Ringel Morris, Percy Liang, and Michael S Bernstein. Generative agents: Interactive simulacra of human behavior. In *Proceedings of the 36th Annual ACM Symposium on User Interface Software and Technology*, pages 1–27, 2023.
- [Park et al., 2024] Joon Park, Tae Jeong, Hyun Kim, Tae Byun, Seung Shin, Kyung Choi, et al. Towards embedding dynamic personas in interactive robots: Masquerading animated social kinematics (mask). arXiv preprint arXiv:2403.10041, 2024.
- [Vaswani et al., 2017] Ashish Vaswani, Noam Shazeer, Niki Parmar, Jakob Uszkoreit, Llion Jones, Aidan N Gomez, Łukasz Kaiser, and Illia Polosukhin. Attention is all you need. Advances in neural information processing systems, 30, 2017.
- [Wasserman and Faust, 1994] Stanley Wasserman and Katherine Faust. Social network analysis: Methods and applications. *Cambridge University Press*, 1994.
- [Wei et al., 2022a] Jason Wei, Yi Tay, Rishi Bommasani, Colin Raffel, Barret Zoph, Sebastian Borgeaud, Dani Yogatama, Maarten Bosma, Denny Zhou, Donald Metzler, et al. Emergent abilities of large language models. *Trans*actions on Machine Learning Research, 2022.

- [Wei *et al.*, 2022b] Jason Wei, Xuezhi Wang, Dale Schuurmans, Maarten Bosma, Brian Ichter, Fei Xia, Ed Chi, Quoc Le, and Denny Zhou. Chain of thought prompting elicits reasoning in large language models. *arXiv preprint arXiv:2201.11903*, 2022.
- [Yang et al., 2023] Joon Sung Yang, Jaemin Kim, and Alice Oh. The emergence of multiagent gpt: Interactive improvisational agents. arXiv preprint arXiv:2308.10236, 2023.
- [Zhang *et al.*, 2023] Sirui Zhang, Zhihong Dong, et al. Metagpt: Meta programming for a multi-agent framework. *arXiv preprint arXiv:2308.00352*, 2023.
- [Zhao et al., 2021] Tony Zhao, Eric Wallace, Shi Feng, Dan Klein, and Sameer Singh. Calibrate before use: Improving few-shot performance of language models. *International Conference on Machine Learning*, pages 12697–12706, 2021.
- [Zhou *et al.*, 2022] Denny Zhou, Nathanael Schärli, Le Hou, Jason Wei, Nathan Scales, Xuezhi Wang, Dale Schuurmans, Maarten Bosma, Ed Chi, Quoc Le, et al. Least-to-most prompting enables complex reasoning in large language models. *arXiv preprint arXiv:2205.10625*, 2022.